DOI 10.1007/s11141-021-10108-5
Radiophysics and Quantum Electronics, Vol. 64, No. 1, June, 2021
(Russian Original Vol. 64, No. 1, January, 2021)

PHYSICS AND MATHEMATICS OF ELECTRIC STREAMERS

N. G. Lehtinen*

UDC 537.5

A streamer is a kind of electric discharge in which there forms a column of ionized matter growing due to the amplified field at its tip. Streamers in air are an important stage of spark discharge, in particular lightning, and constitute sprites (mesospheric discharges). Streamers in large discharges (in sprites, in laboratory experiments with a meter-scale inter-electrode gap and megavolt potential difference, and in lightning) create large branched structures. Microscopic processes, which are responsible for propagation of streamers, are ionization, attachment, electron drift and diffusion, photoionization, and ion processes (detachment, recombination, etc.). Their numerical modeling reproduces the columnar shape of the ionization front, but does not allow to identify the physical and mathematical mechanisms of how the streamer radius and speed are chosen and of branching. A streamer may be described by a finite set of parameters, such as its speed and the radius of its head. The relations between these parameters are known, but do not constitute a complete set of equations: one free parameter (the radius) remains, which defines a streamer "mode" (the terminology is chosen by analogy with small transverse harmonic perturbations of a flat ionization front). As an additional requirement which would give a unique solution, we propose the choice of the most unstable mode that has the maximum speed. Thus, we treat the streamer as a nonlinear instability. This approach yields the results which agree with experimental measurements of streamer speeds, as well as of the streamer propagation threshold field.

This article is prepared based on the material of a lecture presented at the XIX Scientific School "Nonlinear Waves."

1. INTRODUCTION

Streamers are channels of increased ionization in a gas (or a liquid), that advance by ionizing the material in front of them with enhanced field at the streamer tip. Streamers play an important role both in nature and in industry. In nature, they are an important stage of lightning and also constitute Red Sprites (mesospheric discharges). In industry, they may be used to create suprathermal electrons (i.e., those with energies exceeding 1 eV). Streamers in air are especially interesting, and are the subject of this work. They are studied in laboratory discharge experiments with inter-electrode gaps ranging from a few centimeters [1] to several meters. In large laboratory discharges, with a gap of the order of 1 m and voltage of the order of 1 MV, they form complicated branched structures [2, Fig. 8]. The time development of streamer branching in Sprites may be observed with high-frame-rate video cameras.

In long sparks (lightning), one can observe a hierarchy of processes, going from simpler at smaller scales towards larger ones which involve additional physical mechanisms:

* Nikolai.Lehtinen@uib.no

University of Bergen, Bergen, Norway. Translated from Izvestiya Vysshikh Uchebnykh Zavedenii, Radiofizika, Vol. 64, Nos. 1, pp. 12–28, January 2021. Russian DOI: 10.52452/00213462_2021_64_1_12 Original article submitted May 29, 2020; accepted January 28, 2021.

0033-8443/21/6401-0011 © 2021 Springer Science+Business Media, LLC

1. Electron avalanche. A Townsend discharge occurs during this process. One may neglect space charges. Electrons heat up, but transfer their energy to molecules (atoms in inert gases) and ions very weakly.

2. Streamers. When the avalanche grows to a certain scale, the space charges starts to play an important role (this is Meek's criterion) [3]. Electrons are heated (the typical energy is around 3.6 eV), but the molecules remain cold.

3. Leaders. Similarly to streamers, leaders are channel-shaped discharges. The streamers join together and create large current. Neutral molecules are heated up, and strong ionization occurs.

Recently, much attention has been paid to the study of the recently discovered X-ray radiation from electrical discharges. Terrestrial gamma flashes (TGF) were discovered by BATSE instrument at CGRO [4] and were observed later by other, more sensitive, instruments in orbit, such as RHESSI, Fermi, AGILE, ASIM (at a rate of the order of 1 flash per day). They are characterized by duration of the order of 0.1 ms, and total energy greater than or of the order of 1 kJ. They occur simultaneously with lightning and are, presumably, the result of bremsstrahlung radiation which occurs in relativistic runaway electron avalanches. The electrostatic potential scale for such avalanches is 7.4 MeV.

X-rays have been observed also in laboratory experiments, both in positive and negative discharges [5, 6]. Typical photon energies in these reach values of the order of 100 keV. Under these conditions, a relativistic runaway electron avalanche is impossible (the potential drop is insufficient). It is hypothesized that radiation occurs in a process of collisions of streamers or leaders of opposite polarity.

2. PROCESSES IN STREAMERS

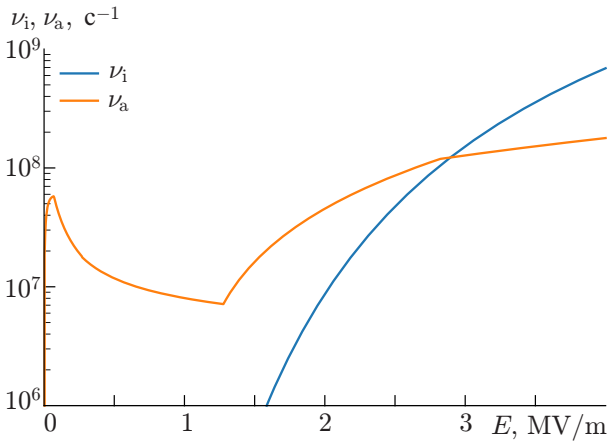

Fig. 1. Most important reactions with participation of electrons in air.

In air, the basic reactions with participation of electrons include impact ionization of N_2 and O_2 molecules, with rate ν_i, and attachment with rate ν_a; dissociative attachment dominates in strong electric fields (it is a two-component process, whose rate is proportional to the atmospheric molecular density N_{atm}), while the three-component attachment is more important at low fields (with rate proportional to N_{atm}^2). We will often use effective ionization rate

$$\nu_t(E) \equiv \nu_i(E) - \nu_a(E)$$

These and other processes are described in detail, e.g., in [7, Ch. 2]. In Fig. 1 we show typical dependencies of ν_i and ν_a on electric field [8].

Intersection field $E_k \approx 3$ MV/m, at which $\nu_t = \nu_i - \nu_a = 0$, is often called critical field and confused with breakdown field. We must keep in mind the following.

1) In a Townsend discharge, which occurs in steady-state conditions, electron detachment from negative ions plays an important role. This may make the discharge possible at $E < E_k$.

2) The minimal field, at which a streamer discharge is possible in a finite gap, is calculated with the help of Meek's criterion and may be $E > E_k$, especially for smaller gaps.

Propagation of a streamer ionization front is made possible by the following mechanisms.

1) Electron drift (forward for a negative streamer) with speed $\mathbf{v} = -\mu(E)\mathbf{E}$, where $\mu \approx 0.04$–0.05 m^2/(V · s) is the electron mobility at typical fields in streamers (with values exceeding 1 MV/m). We note that at low fields the mobility is higher by an order of magnitude.

2) Electron diffusion (in the absence of photoionization), with coefficient $D \approx 0.1$ m^2/s.

3) Photoionization (the main mechanism in air). Photons in UV range with wavelengths $\lambda = 980$–1025 Å are produced by collisions of electrons with nitrogen N_2, then propagate forward of the streamer

and ionize oxygen O_2:

$$e^- + N_2 \to e^- + N_2^*;$$
$$N_2^* \to N_2 + h\nu(980\text{–}1025\ \text{Å});$$
$$h\nu + O_2 \to O_2^+ + e^-.$$

The streamer propagation mechanism was first proposed by the authors of book [3]. The photons originating in the streamer head are radiated forward of the streamer and produce ionization. The newly created electrons serve as seeds of ionization avalanches in the high field of the streamer head. These avalanches are formed as a result of impact ionization, grow in the backward direction and merge with the streamer. This mechanism works for both positive (cathode-directed) and negative streamers [9, p. 335, 338]. In negative streamers, even though the photon-initiated avalanches grow forward in the laboratory reference frame, the streamer catches up with them. In the reference frame of the streamer head, the avalanches grow backwards, similarly to positive streamers.

The streamer parameters, such as its speed and transverse size (radius), can be measured experimentally. One may also use numerical modeling, in which the microscopic physics equations are solved (under condition that the numerical methods are stable and accurate). Examples of such methods, which use extensive computational resources, include adaptive mesh refinement (AMR) three-dimensional hydrodynamic models [10] and particle-in-cell (PIC) methods [11]. However, so far, these computations incur significant errors (of the order of 10%, judging by examples in [12]), due to numerical inaccuracies and instabilities. Results related to streamer branching are especially unreliable [13, p. 291]. Moreover, these numerical experiments, even though they may reproduce the laboratory-experiment results, cannot answer the question about the physical mechanisms which determine the streamer radius and speed.

The question about these mechanisms had been faced by physicists for many years [14]. We can cite [7, p. 46–47]: "The mechanisms by which a plasma conductor acquires a definite [...] radius [...] seem to go far beyond the steady state processes [...] We should recognize that these mechanisms are not quite clear at present."

The scientists who proposed the streamer mechanism [3] also assumed that the initial streamer radius is determined by the transverse spreading of electrons in an avalanche as a result of diffusion. This prompted many authors to explore the idea that electron diffusion determines the streamer radius during its propagation as well [15, 16, 17]. We may estimate, however, that the increase in the streamer radius due to diffusion is much slower than that observed in laboratory and numerical experiments. The transverse size of a flow of directed velocity V diffusing with coefficient D grows as $\sqrt{DL/V}$ with distance L. Substituting the typical values $L \approx 0.1$ m, $V \approx 10^6$ m/s, and $D \approx 0.1$ m^2/s for a laboratory streamer in air, we get a transverse size increase of less than or of the order of 0.1 mm, while typically observed radii are in excess of 1 mm (see, e.g., [18, 19, 20]). Moreover, it was argued in [21] that diffusion may be completely neglected in the approximate analysis of regular streamer propagation.

3. PARAMETRIC MODEL OF A STREAMER

Let us write down the hydrodynamic equations for electric discharge in air (see, for example, [8, 22]):

$$\frac{\partial n}{\partial t} = -\nabla\cdot(\mathbf{v}n) + \nabla\cdot(D\nabla n) + (\nu_\mathrm{i} - \nu_\mathrm{a})n + \nu_\mathrm{d} n_- - \beta n n_+ + s_\mathrm{p};$$
$$\frac{\partial n_+}{\partial t} = \nu_\mathrm{i} n - (\beta n + \beta_- n_-)n_+ + s_\mathrm{p}; \qquad \frac{\partial n_-}{\partial t} = \nu_\mathrm{a} n - \nu_\mathrm{d} n_- - \beta_- n_+ n_-;$$
$$\nabla\cdot\mathbf{E} = \frac{e}{\varepsilon_0}(n_+ - n - n_-). \tag{1}$$

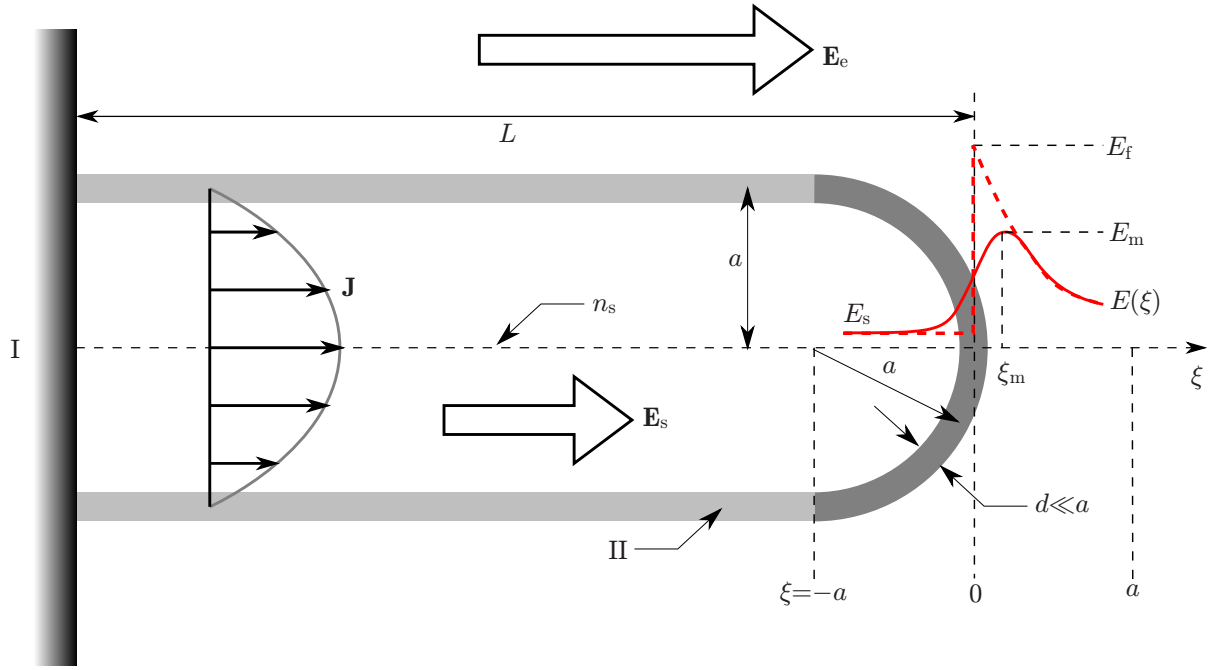

Fig. 2. Streamer model (I — ideally conducting plane, II — positively charged surface). The field directions are for a positive streamer (for a negative one they are opposite). Solid and dashed red lines the sketch $E(\xi)$ dependence for a streamer with finite ionization front thickness d, and infinitely thin front ($d = 0$), respectively.

Here n, n_+, n_- are the number densities of electrons, the positive and negative ions, respectively, ν_i, ν_a, ν_d, and β, β_- are the coefficients determining the rates of ionization, attachment, detachment, electron-ion recombination and ion-ion recombination, respectively, and s_p is photoionization given by Eq. [23]:

$$s_\mathrm{p}(\mathbf{r}) = \int CF(|\mathbf{r}-\mathbf{r}'|)\nu_\mathrm{i}(|\mathbf{E}(\mathbf{r}')|)n(\mathbf{r}')\,\mathrm{d}^3\mathbf{r}'.$$

The nonlocality of photoionization is described by the kernel, normalized to unity:

$$F(r) = \frac{\exp(-r/\Lambda_2) - \exp(-r/\Lambda_1)}{4\pi r^3 \log(\Lambda_2/\Lambda_1)}, \qquad \Lambda_2 \approx 2 \text{ mm}, \Lambda_1 \approx 35\ \mu\text{m}. \tag{2}$$

Coefficient C characterizes the efficiency of photoionization; $C \approx 0.01$ at sea level and depends on the air density. System (1) was solved numerically in [22].

Further, to simplify the problem, we will keep only processes which are important for the description of a streamer, and will neglect the following: nonlocal electron transport effects, electron diffusion, ion motion, electron detachment, recombination, and inter-ion processes. Next, we simplify these equations for a specific system consisting of an electrode and a discharge, and the shape of the ionization front shown in Fig. 2. This system is parameterized by a finite, or, at least, a very limited set of parameters compared with system (1).

In the diagram shown in Fig. 2 the symmetry axis is parallel to the external constant field $\mathbf{E}_\mathrm{e}$. The streamer is attached to the perpendicular ideally conducting electrode. The part of electrode surface occupied by the streamer absorbs electrons in the positive streamer case and is an ideal electron emitter in the negative streamer case.[1] The streamer of full length L consists of the head (a hemisphere of radius a) attached to the channel (a cylinder of the same radius). The internal part carries uniform channel field $\mathbf{E}_\mathrm{s}$,

[1] Electrode processes are the subject of future research.

which is smaller than the external field. The electron number density n is positive inside the streamer and falls off to $n = 0$ outside, and at the forward boundary of the streamer this drop is steep, with the scale of front thickness $d \ll a$. We assume that n is uniform inside the channel along its axis and denote it as n_s (but n may gradually fall off towards the side walls). The assumption of uniformity of $\mathbf{E}_\mathrm{s}$ and n_s, probably, contributes the biggest part to the error in the described model, which may be of the order of a few tens of percent, because n drops inside the channel due to electron attachment, which is neglected in the model.

The streamer grows (propagates) along x-axis with velocity $V \equiv \mathrm{d}L/\,\mathrm{d}t$. We assume that the head is in a steady state in its own reference frame, which allows us to write equations in terms of co-moving coordinate $\xi = x - Vt$. It is convenient to take as the origin of ξ any point within the front boundary of the streamer, as is shown in Fig. 2. The streamer propagates by ionizing air in front of itself with a high electric field with maximal value E_m (the field is shown schematically by a solid red line in Fig. 2).

Beside E_m, it is useful to introduce another field E_f, which is the field that the streamer would create in the case of an infinitely thin ionization front ($d = 0$), but with the same surface charge density at the streamer boundary (the distribution of such a field is shown by a dashed red line in Fig. 2). Modeling shows that $E_\mathrm{m}/E_\mathrm{f} \approx 0.7$–$0.85$. Approximately the same field E_f would be obtained in the case of a flat ionization front, considered in Sec. 4.3. In order to find relations between streamer parameters and to perform subsequent practical calculations, it is more convenient to choose E_f as one of the independent parameters instead of E_m and to calculate E_m afterwards on the basis of known E_f and thickness d.

Thus, we have chosen several parameters (a, V, E_s, E_f and n_s), which fully (even though approximately) describe our system. We emphasize that E_e and L are the given external values: E_e is determined by the laboratory conditions and $L = \int V\,\mathrm{d}t$, by the streamer propagation history. In the next section, we will write down equations which relate these parameters to each other.

We should mention that this is not the first attempt of a similar streamer description. A parametric model was considered, e.g., by [24]. However, because the equation are rather complicated, in such models it is hard to notice internal inconsistencies (overdefined system of equation) or insufficiency of the system (dependent equations).

4. SYSTEM OF ALGEBRAIC EQUATIONS

We have identified the following relationships between the parameters:

1) Electrostatic relationship between fields E_s E_e, E_f (E_m), which can be calculated by the method of moments if we assume that all the charges are approximately concentrated on the streamer surface (i.e., we neglect the thickness d).

2) Continuity of the total current at the tip of the streamer: the conductivity current in the channel becomes the displacement current outside the streamer.

3) The balance of ionization time and the relaxation time in the channel.

4) The balance between the processes of impact and photo ionization [25].

Let us consider each of them in detail.

4.1. Equation 1: Fields

The external uniform constant field $\mathbf{E}_\mathrm{e}$ is fixed by the laboratory conditions. Inside the channel, the conductivity is high, and there is a field $\mathbf{E}_\mathrm{s}$, such that $0 < E_\mathrm{s} < E_\mathrm{e}$. The field at the front boundary can be estimated by the reasoning given in [7, p. 78]: the potential at the streamer tip differs from the undisturbed one by $\Delta U = L(E_\mathrm{e} - E_\mathrm{s})$, and the field is approximately $E_\mathrm{f} = \Delta U/a$. The field E_f can be calculated more accurately by utilizing the method of moments [26, Ch. 2].

The field in front of the streamer falls off approximately as

$$E(\xi) = E_\mathrm{e} + \frac{E_\mathrm{f} - E_\mathrm{e}}{1 + \xi/\ell}, \qquad d \lesssim \xi < a, \tag{3}$$

where $\ell \approx (0.3\text{–}0.4)a$ is the field width [21]. In Sec. 4.6, we give the approximate formula for ℓ, fitted from the method-of-moment results.

4.2. Equation 2: Current continuity

There is a conductivity current flowing along the streamer channel with density $J_\mathrm{c} = en_\mathrm{s}\mu(E_\mathrm{s})E_\mathrm{s}$. The electron number density falls off steeply (with the scale of the front thickness $d \ll a$) to zero at the front boundary of the streamer. The density of full current $J = J_\mathrm{c} + J_\mathrm{d}$, consisting of conductivity current J_c and displacement current $J_\mathrm{d} = \varepsilon_0 \partial E/\partial t$, must remain approximately constant ($\nabla\cdot\mathbf{J} = 0$ from Maxwell equations, ε_0 is the dielectric constant). By using the property of the co-moving coordinate $\partial E/\partial t = -V\partial/\partial\xi$ and the expression for the field (3), we find

$$J_\mathrm{d}(\xi) = \frac{\varepsilon_0 V(E_\mathrm{f} - E_\mathrm{e})}{\ell(1+\xi/\ell)^2}.$$

At small $\xi \sim d$, neglecting $d \ll \ell$ and equating this expression to the conductivity current density in the channel, we get the equation for the current continuity [27].

The total current J is approximately equal to J_d at $\xi > 0$ and $J_\mathrm{c} = J_\mathrm{d}(0)$ at $\xi < 0$.

Let us note that J_d falls off as the inverse square of the distance. Physically, this may be interpreted as isotropic divergence of the displacement current away from the streamer tip. The integrated diverging displacement current must be equal to the total current in the streamer channel. Also it is worth noting that inside the ionization front (at the tip) conductivity and displacement current densities vary significantly, so that each of them exceeds the total current density (their sum).

4.3. Equation 3: Ionization front

Hydrodynamic equations (1) can be rewritten as

$$\varepsilon_0 \partial_t \mathbf{E} = e\mathbf{v}n + \mathbf{J}, \qquad \partial_t n + \nabla\cdot(\mathbf{v}n) = \nu_\mathrm{t} n + s_\mathrm{p}. \tag{4}$$

Herewith, $\partial_\alpha \equiv \partial/\partial_\alpha$. Neglecting photoionization s_p, for a flat steady-state front advancing with speed $V > 0$ we get one-dimensional equations ($\partial/\partial y, \partial/\partial z \equiv 0$)

$$-\varepsilon_0 V \partial_\xi E = -evn, \qquad -\partial_\xi([V \pm v]n) = \nu_\mathrm{t} n,$$

where $v = |v_x| = \mp v_x > 0$ (the upper sign for the positive and the lower for the negative front). The current $J = \mathrm{const} = 0$, because it is absent far ahead of the front ($\xi \to +\infty$), where the field is constant and is equal to the external field $E_\mathrm{f} = E(\xi \to +\infty)$. From $J = 0$ it follows also that $E = 0$ at $\xi \to -\infty$. This is different from a streamer, in which $J > 0$ and $E(-\infty) = E_\mathrm{s} > 0$. Divide the second equation by the first:

$$\frac{e}{\varepsilon_0}\frac{\mathrm{d}}{\mathrm{d}E}\left[\frac{(V \pm v)n}{V}\right] = \frac{\nu_\mathrm{t}}{v} \equiv \alpha_\mathrm{t}(E).$$

Upon integration, we get

$$\frac{en(E)}{\varepsilon_0} = \frac{V}{V \pm v}\int_E^{E_\mathrm{f}} \alpha_\mathrm{t}(E)\,\mathrm{d}E. \tag{5}$$

Here, α_t is the effective Townsend coefficient. The Maxwellian relaxation rate far behind the front (where $E = 0$) is

$$\tau_M^{-1} = \frac{\sigma_\mathrm{s}}{\varepsilon_0} = \frac{en_\mathrm{s}\mu_0}{\varepsilon_0} = \mu_0 \int_0^{E_\mathrm{f}} \frac{\nu_\mathrm{t}(E)}{\mu E}\,dE \sim \nu_\mathrm{t}(E_\mathrm{f}),$$

where $\mu_0 = \mu(E = 0)$ and $n_\mathrm{s} = n(E = 0)$ is the electron number density far behind the front, at $\xi \to -\infty$. The last expression describes an approximate balance of the time scales of ionization and relaxation, which may be interpreted as the criterion of propagation stability of a front or a streamer [28].

After substitution of the found $n(E)$ into either of equations, we may find the spatial dependence $n(\xi)$, $E(\xi)$. As an example, take $\nu_t(E) = KE, v = 0$. Then the front has the shape of a sigmoid (logistic) curve, with width $d = V/\nu_t(E_f)$, shown in Fig. 3, i.e., $n(\xi) = n_s[1 - S(\xi)]$, $E(\xi) = E_f S(\xi)$, where

$$S(\xi) = \frac{1}{1 + \exp(-\xi/d)}. \tag{6}$$

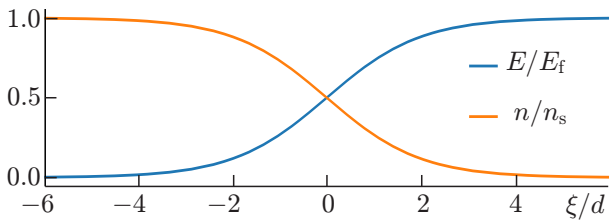

Fig. 3. Solution $n(\xi), E(\xi)$ for a flat ionization front, for the case $\nu_t(E) = KE, \mu = 0$.

The speed V of the flat front can be found from the boundary conditions at $\xi \to \infty$ (ahead of the front), for different mechanisms of its propagation. The possible values of V satisfy inequality $V > V_0$, where V_0 is defined by one of the following formulas.

1) When $\mu > 0$ and $D > 0$,

$$V_0 = \mp\mu(E_f)E_f + \sqrt{2D\nu_t(E_f)}$$

(Kolmogorov-Petrovskii-Piskunov formula [29, p. 77]).

2) In the presence of photoionization, but with $D = 0$ [29, Eq. (3.1.85)]:

$$V_0 = \mp\mu(E_f)E_f + \nu_t(E_f)\Lambda_{max}$$

Here and below the upper (lower) sign is for a positive (negative) ionization front. Unfortunately, these expressions are only valid for a flat front and cannot be applied to streamers. Also, we will show that streamer V has only a single valid value, in contrast to the inequality above.

The expressions derived in the flat ionization front theory can be found in an excellent detailed review [29].

4.4. Equation 4: Photoionization balance

Let us consider the balance between two processes: photoionization (caused by photons radiated forward) and impact ionization (caused by backward avalanches).

The photon source is the streamer front near the tip, where ionization is actively produced. We assume that this active region has approximately the spatial shape of a disk with radius $a_{ph} \sim a$. For calculations in this paper, we took $a_{ph} = a/2$, but the results change little if one takes, for example, $a_{ph} = a$. The number of photons is proportional to the number of electrons created in the process of ionization, i.e., the number density of electrons in the streamer channel n_s. The photons fly forward and create seeds for avalanches at a distance $\xi_p \sim a_{ph}$ ahead of the front with number density n_p.[2]

The resulting avalanches grow exponentially in the backward direction, towards the streamer. The growth rate, however, is not the usual Townsend coefficient $\alpha_t = \nu_t/v$, but a "Doppler-shifted" coefficient $\alpha_{eff} = \nu_t/(V \pm v)$. The inverse of α_{eff} is the front thickness $d = (V \pm v)/\nu_t$. We emphasize that, since streamer speed V exceeds the electron drift speed v, the sign of d is always positive not only for positive streamers (upper sign), but also for negative streamers (lower sign). This also means that the avalanches always grow backward towards the streamer in the reference frame associated with its head.

Loeb [30] was the first to obtain the formula relating streamer speed to its radius: from the exponential growth we have $\log(n_s/n_p) = \alpha_{eff} a$, hence

$$V \pm v = \frac{a\nu_t(E_f)}{\log(n_s/n_p)}.$$

[2] The photons, of course, are flying in all directions, but the region we consider here is most important, because it has a high electric field and there were no free electrons there before the photon arrival.

The still unknown value of $\log(n_s/n_p)$ can be taken to be approximately 8 [21]. By solving strictly the second equation of system (4), one may obtain a more accurate expression [25], which is given in Sec. 4.6 (however, in a slightly different form, since we assumed the photon source to have a disk shape). From this equation one can also estimate, in particular, the distance ξ_p to the region important for photoionization.

4.5. Discussion of approximations used

4.5.1. Streamer shape

We assumed that the streamer channel radius is constant along its length and is equal to the head radius. However, the streamer channel radius may be different from the curvature radius of the head. For example, the hydrodynamic calculations [31] showed that it is greater by a factor of two in positive and by a factor of three or more in negative streamers. If $E_s = \text{const}$, then variations of the channel radius far from the head will not strongly affect the field ahead of the streamer, $E(\xi > 0)$, because it is formed mostly by surface charges near the tip. Thus, parameter a entering our equations best describes the curvature radius of the head than, e.g., the maximum radius of the channel.

4.5.2. Non-uniformity of n_s and E_s along the channel

In expression (3) we assumed that the field inside the channel $E_s = \text{const}$. The current continuity along the channel requires that $n_s v(E_s) = \text{const}$, which means that $E_s = \text{const}$ necessarily implies $n_s = \text{const}$. The assumption of uniformity of E_s and n_s along the channel, however, will be invalid if we take into account the processes of attachment and recombination in the channel (we touch upon this topic in Sec.7̃). However, even when we neglect these processes, n_s may be non-uniform due to the history of the streamer development: different parts of the streamer were created at different conditions (namely, streamer lengths) and, therefore, may have different local values n_s.[3] Peeking ahead, we see in Fig. 5*e* and 6*e* that n_s can vary significantly as the streamer grows. We make an error by substituting non-uniform value n_s in the channel with its value from the last added part of the streamer. This error may be of the order of a few tens of percent and is possibly the biggest contribution to the total error in the presented calculations.

4.5.3. Head curvature and finite current $J \neq 0$ through the front

Expression (5), relating electron number density in the ionization front with the field ahead of the streamer, will change when we substitute expression for J found in Sec. 4.2 into Eq. (4). Solution of the obtained equation is beyond the scope of the present work and deserves a separate discussion. In particular, we are going to obtain an expression for the field different from (3) inside the front, at $|\xi| \lesssim d$ (represented by a solid red line in Fig. 2). If the gradual transition from field $E(\xi) = E_s$ at $\xi \lesssim -d$ to expression (3) at $\xi \gtrsim d$ is approximately described by the sigmoid (logistic) curve (6), then the maximum field E_m is equal to

$$E_m = E_f \left[1 - \frac{d}{\ell} \log\left(\frac{\ell}{d}\right)\right]$$

It is less than E_f and is achieved at $\xi = \xi_m = d \log(\ell/d)$. One must do additional calculations in order to estimate the relative error in the expression for n_s. Unlike $E(-\infty) = 0$ for the flat front, we have $E(\xi \lesssim -d) = E_s > 0$, which, at least, gives a different lower integration limit in expression (5). Thus, expression (5) is approximate, but remains accurate up to the order of magnitude.

4.6. System of algebraic equations for a, V, E_s, E_f, and n_s

In this Section we compiled all the equations for the reader's convenience.

[3] We can neglect electron drift inside the channel compared to the streamer speed, $v(E_s) \ll V$.

1) Relation between electric fields, given by electrostatic distribution of charges on the streamer surface (analytical approximation of the results of method-of-moments calculations) [7, p. 78] (connection between E_s and E_f):

$$E(\xi) \approx \left[2 + 0.56(2L/a)^{0.92}\right] \frac{E_\mathrm{e} - E_\mathrm{s}}{1 + \xi/\ell} + E_\mathrm{e}, \qquad E_\mathrm{f} = E(0), \qquad \frac{\ell}{a} \approx 0.40 - \frac{0.59}{(L/a) + 2.31},$$

where ℓ is the width of the electric field [21].

2) Continuity of the full electric current through the streamer front [27] (connection between E_s, n_s and V):

$$J_\mathrm{c} = \varepsilon_0 \left.\frac{\partial E}{\partial t}\right|_{\xi=0} \qquad \Longrightarrow \qquad e n_\mathrm{s} v(E_\mathrm{s}) = \frac{\varepsilon_0 V (E_\mathrm{f} - E_\mathrm{e})}{\ell},$$

where v is the electron drift speed.

3) Criterion of streamer propagation stability, obtained from the theory of the flat ionization front [29, Ch. 3] (connection between n_s and E_f):

$$n_\mathrm{s} = \frac{\varepsilon_0}{e} \int_0^{E_\mathrm{f}} \frac{\nu_\mathrm{t}(E')}{v(E')}\, dE',$$

where ν_t is the effective ionization rate. This relation is approximately equivalent to $\tau_M \sim \tau_\mathrm{ion} = 1/\nu_\mathrm{t}(E_\mathrm{f})$.

4) Connection between the speed and the radius, determined by photoionization [25, Eq. 17] (connection between V, E_f and a):

$$\int_0^\infty S_\mathrm{ph}(\xi) \exp\left[\int_0^\xi \frac{\nu_\mathrm{t}(E)\, d\xi'}{V \pm v(E)}\right] d\xi = 1,$$

S_ph is the source of photoionization electrons per unit n_s, created by the processes occurring in the front of radius $a_\mathrm{ph} = a/2$:

$$S_\mathrm{ph}(\xi) = \int_{r_\perp < a_\mathrm{ph}} CF(r)\, d^2\mathbf{r}_\perp, \qquad r = \sqrt{\xi^2 + r_\perp^2}$$

where $F(r)$ is given by Eq. (2).

5. DISPERSION FUNCTION

After a careful look at the obtained system of algebraic equations we notice that, at fixed external conditions E_e and L, it does not have a single-valued solution, because the number of equations is less by one than the number of unknown parameters. Thus, there remains one free parameter, which we can choose to be, e.g., the radius a. Then we obtain solutions $V = V(a)$, $E_\mathrm{s} = E_\mathrm{s}(a)$, and so on.

Let us draw an analogy with another problem, which has a similar goal: finding small perturbations of a flat ionization front. This problem was tackled in detail by [32] (however, only electron drift and diffusion were taken into account, but not photoionization). It was found that in the linear approximation there is an instability: small perturbations, proportional to $\cos(ky)$, grow as $\exp(st)$ with growth rate s, which is a function of the transverse wave number k. Function $s(k)$ is called the dispersion function. When we solve the problem of growth of small perturbations, it is obvious that k is a free parameter. This explains the fact that in our problem which concerns a long streamer, even though it is nonlinear, the transverse size a also turned out to be the free parameter. The set of various parameters of a small harmonic perturbation (e.g., the change in the field at the protrusions in proportion to the amplitude, etc.) may be called a "mode" (analogously to an electromagnetic mode in a waveguide). We may also call the set of parameters $\{V(a), E_\mathrm{s}(a), \dots\}$ at fixed radius a a streamer mode.

Evolution of small perturbations of a flat front depends on the initial conditions. If in the beginning

there is a combination of perturbations with various k, then the perturbation which corresponds to the maximum of the dispersion function $s(k)$ grows the fastest and in the long term only it will "survive," i.e., after some time we will see only the perturbation proportional to $\cos(k^* y)$, where $\max_k s(k) = s(k^*)$. This solution (and the scale k^*) is preferred as the most unstable. We may assume that, also in our case, there is a preferred most unstable solution which determines the real streamer radius, as well as all of its other parameters. Identification of such a solution is complicated by the fact that our problem is nonlinear and the growth rate $s(k)$ does not exist. The following reasoning will help find the fitting analogy.

In the linear harmonic perturbations of a flat front, the protrusion size L (we use this notation because the protrusion size is analogous to the streamer length in our problem) grows as $L = L_0 \exp[s(k)t]$, and the speed of the protrusions (in respect to the speed of the overall front) $V = \mathrm{d}L/\,\mathrm{d}t = s(k)L$. Thus, the speed plays the same role as $s(k)$ at fixed L, and we may call the found dependence $V(a)$ the dispersion function of the streamer. The most unstable (preferred) solution corresponds to $a = a^*$, where $\max_a V(a) = V(a^*)$. This solution is the preferred mode which determines the real streamer parameters which are obtained in laboratory and numerical experiments.

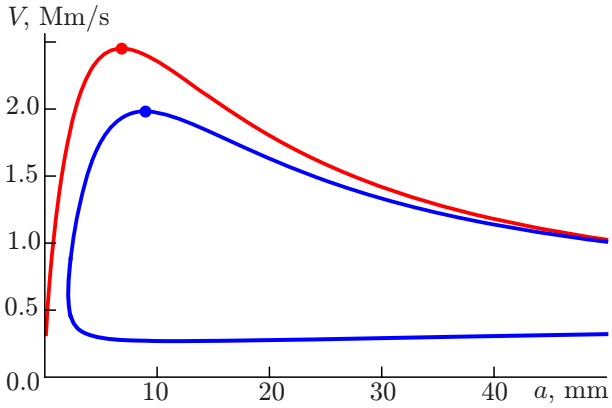

Fig. 4. An example of calculated dispersion functions $V(a)$ for streamers in dry air at sea level for the external field $E_\mathrm{e} = 1.5$ MV/m and streamer length $L = 80$ mm. Positive streamers (red curve) have a single solution for all a, while negative (blue curve) have zero or two solutions. The large dot denotes the maximum V.

Our assumption that the mode with maximal speed determines the parameters of a streamer observed in nature is heuristic, and we cannot yet find its strict mathematical justification, because the modes under consideration are nonlinear and do not allow a mode combination, which was possible in the linear problem concerning small perturbations of a flat front. Let us note that [33, Fig. 1] also suggested (at a heuristic level) that when the streamer changes its radius to the value best corresponding to the physical conditions, the speed may increase. However, the authors of that work did not use the maximization of speed for a numerical solution.

Selection of the preferred radius by the maximization of velocity can be used in one-dimensional streamer models, such as the one suggested by [34]. Those authors used the constant-radius assumption and noted that the modeling results strongly depended on the choice. The algorithm that we suggest will allow to choose a more physical, i.e., non-constant, radius value.

An example of calculated dispersion functions for streamers of both polarities is shown in Fig. 4. The large dot denotes the preferred mode, i.e., the real streamer speeds and radii.

6. CALCULATION RESULTS

The calculations were performed for streamers in dry air at sea level. Expressions for electron mobility and ionization and attachment rates were taken from [8, 35]. Calculations were performed for streamer lengths in interval $L = 5$–200 mm with step 5 mm and external fields in interval $E_\mathrm{e} = 0.1$–3 MV/m with step 0.05 MV/m. Usually, the calculated dispersion function had one branch for positive streamers and two branches for negative ones, as is shown in Fig. 4. The top branch $V(a)$ always had one local maximum, while all the other calculated parameters (E_s, E_m, n_s) were monotonic functions of a. The results presented below correspond to the maximum of $V(a)$, i.e., to the most unstable solution (the preferred mode).

The positive streamer results are presented in Fig. 5. The speed is shown in comparison with laboratory measurements [1], which were performed under conditions very similar to those in our model (i.e., with an approximately constant and uniform field). A convenient unit for measuring streamer speed is 1 Mm/s= 10^6 m/s=1 mm/ns. We also get good agreement (within 30%) with the numerical experiment [12] in which hydrodynamic equations were solved (these results are not presented here).

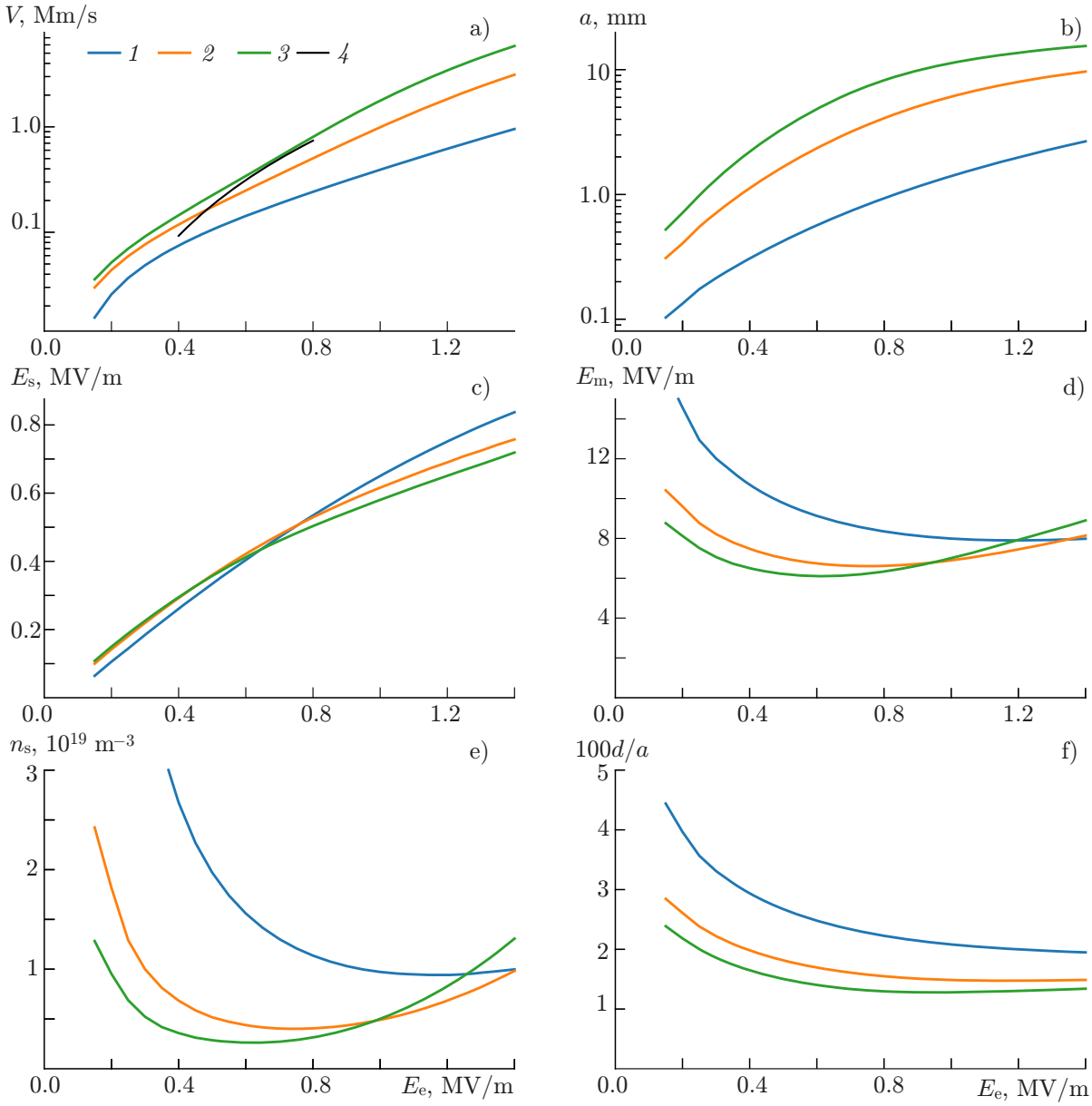

Fig. 5. Results for positive streamers as functions of external field E_e, for three different values of $L = 40$ mm (curves *1*); 120 mm (*2*), and 200 mm (*3*): velocity V (*a*), radius a (*b*), field inside the streamer E_s (*c*), maximum field E_m (*d*), electron number density inside the channel n_s (*e*), front thickness d as a fraction of radius a in percent (*f*). Results of laboratory measurements [1, Fig. 10] at $L = 120$ mm are also shown (*a*, curve *4*).

The negative streamer results are presented in Fig. 6. Some plots have a completely different shape than in the positive streamer case. In particular, the solution starts only from finite E_e (for fixed L).

7. THRESHOLD FIELDS

Attachment and recombination in the streamer channel decrease its conductivity, which causes electrical detachment of the streamer from the electrode, i.e., the breaking of the electrical circuit. The current through the streamer stops, and, presumably, the streamer also stops. Thus, this mechanism determines the threshold field for positive streamers.

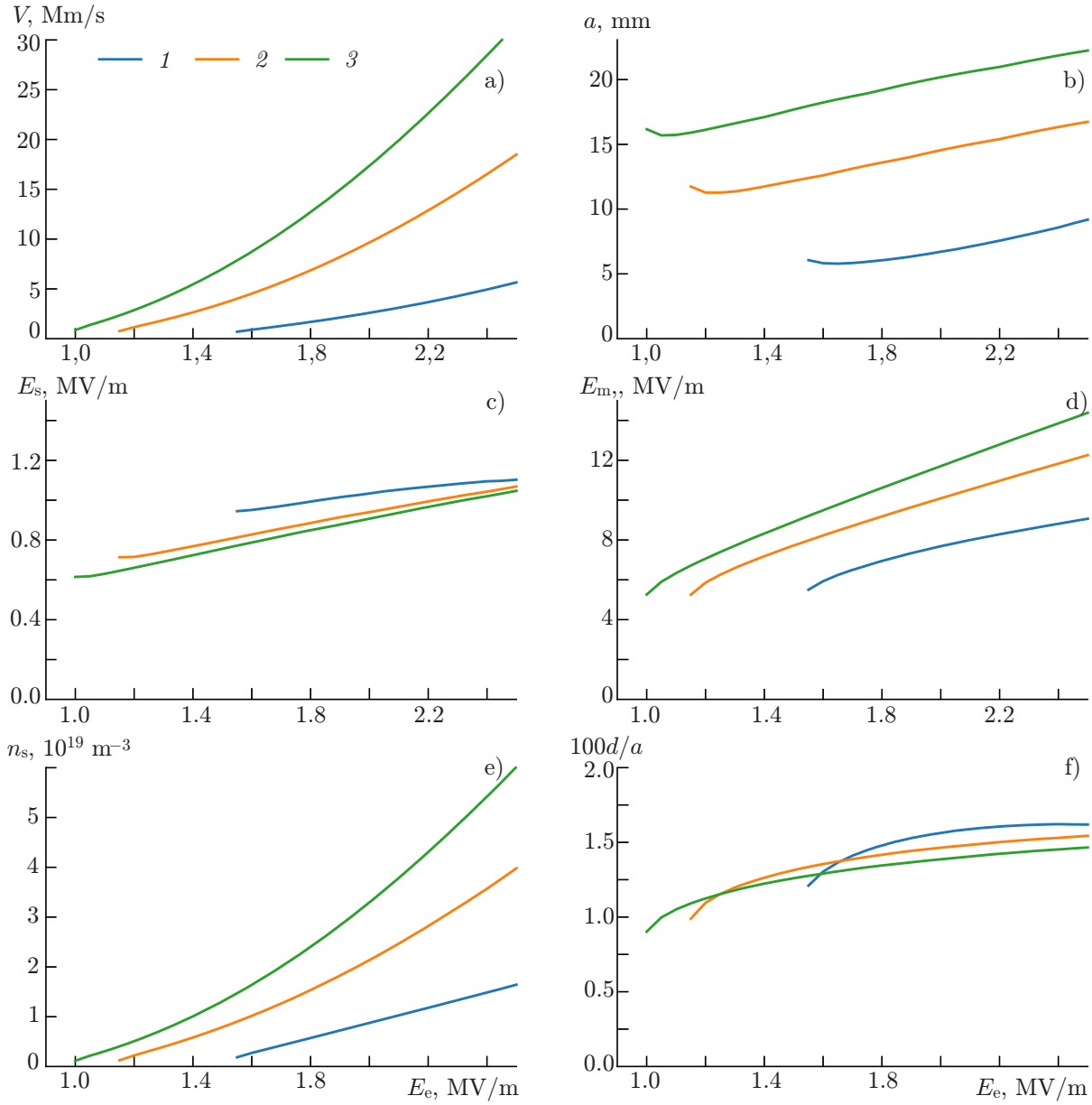

Fig. 6. Results for negative streamers as functions of external field E_e, for three different values of $L = 40$ mm (curves *1*); 120 mm (*2*), and 200 mm (*3*): velocity V (*a*), radius a (*b*), field inside the streamer E_s (*c*), maximum field E_m (*d*), electron number density inside the channel n_s (*e*), front thickness d as a fraction of radius a in percent (*f*).

It should be noted that it had been hypothesized that a streamer may exist separately from an electrode. For example, [36, Fig. 22*b*] describes a unipolar streamer soliton with a "compensation zone" behind the streamer, in which both conductivity and charge per unit length gradually fall off to zero.

The field inside the channel is much lower than the intersection field E_k. In such a field, the main role is played by the three-component attachment (for computations taken from [8]). The electron number density drops by factor $K = e^{-L/L_{att}}$, where the characteristic scale along the channel, at which the attachment occurs, is

$$L_{att} = \frac{V \pm v(E_s)}{\nu_a(E_s) - \nu_i(E_s)}.$$

Fields corresponding to a given factor K are plotted in Fig. 7, for a range of streamer lengths. For comparison, we plotted the experimental data for threshold field E_{+t}, obtained in [1]. The electron number density drop which corresponds best to the experimental data is rather strong, $K \approx 10^{-5}$. It is possible that detachment, which we neglected, reduces the role of attachment, and slows down the drop in the electron number density.

The mechanism of threshold field for negative streamers is completely different. As we saw in Fig. 6, the solution disappears at low values of external field E_e. Values of E_{-t} at which this occurs are also plotted in Fig. 7, and agree with experimental values $E_{-t} = 0.75$–1.25 MV/m [9, p. 362].

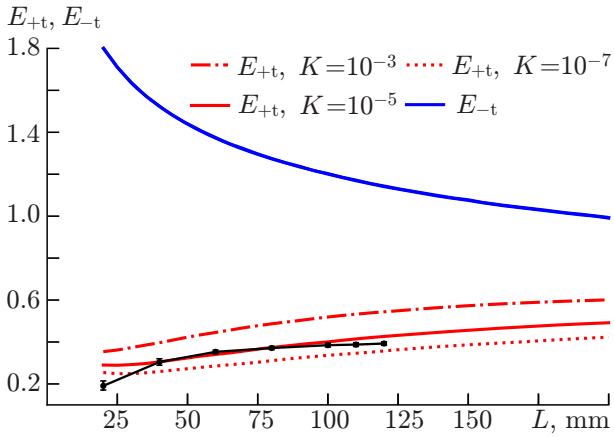

Fig. 7. Threshold fields E_{+t} and E_{-t} for positive and negative streamers as functions of length L. Experimental data (black curve) are taken from [1, Fig. 4].

8. CONCLUSIONS

We have shown the following.

1) A streamer discharge in field E_e of length L can be described by a system of algebraic equations, solving which one obtains "modes" at different radii a.

2) By maximizing the speed of the streamer front V, one obtains the preferred solution, which is realized physically.

3) The calculated streamer parameters agree with experimental results and hydrodynamic models.

4) Threshold fields are functions of streamer length L, and their physical causes are different for positive and negative streamers. The negative streamer threshold is compatible with the experimental values $E_{-t} \approx 0.75$–1.25 MV/m [9, p. 362], while the positive streamer threshold in our model is compatible with the experimental value $E_{+t} \approx 0.45$ MV/m only if one assumes an underestimated value of the attachment coefficient.

This study was supported by the European Research Council under the European Union's Seventh Framework Programme (FP7/2007-2013)/ERC grant agreement No. 320839 and the Research Council of Norway under contracts 208028/F50, 216872/F50 and 223252/F50 (CoE).

APPENDIX

The Python3 code which may be used to reproduce the calculations described here, and instructions for its use, are available at https://gitlab.com/nleht/streamer_parameters. An example of system 1 solution in [22], with a collision of streamers of opposite polarities, is available as a video at https://www.youtube.com/watch?v=xbaDeLYERkQ .

REFERENCES

1. N. L. Allen and P. N. Mikropoulos, *J. Phys. D: Appl. Phys.*, **32**, No. 8, 913–919 (1999). https://doi.org/10.1088/0022-3727/32/8/012
2. P. O. Kochkin, A. P. J. van Deursen, and U. Ebert, *J. Phys. D: Appl. Phys.*, **47**, No. 14, 145203 (2014). https://doi.org/10.1088/0022-3727/47/14/145203
3. L. B. Loeb and J. M. Meek, *The Mechanism of the Electric Spark*, Stanford University Press, Stanford University, California, (1941).

4. G. J. Fishman, P. N. Bhat, R. Malozzi, et al., *Science*, **264**, 1313–1316 (1994). https://doi.org/10.1126/science.264.5163.1313
5. P. O. Kochkin, C. V. Nguyen, A. P. J. van Deursen, and U. Ebert, *J. Phys. D: Appl. Phys.*, **45**, No. 42, 425202 (2012). https://doi.org/10.1088/0022-3727/45/42/425202
6. P. O. Kochkin, A. P. J. van Deursen, and U. Ebert, *J. Phys. D: Appl. Phys.*, **48**, No. 2, 025205 (2015). https://doi.org/10.1088/0022-3727/48/2/025205
7. E. M. Bazelyan and Y. P. Raizer, *Spark Discharge*, CRC Press, New York, (1998).
8. R. Morrow and J. J. Lowke, *J. Phys. D: Appl. Phys.*, **30**, 614–627 (1997). https://doi.org/10.1088/0022-3727/30/4/017
9. Y. P. Raizer, *Gas discharge physics*, Springer, Berlin (1991).
10. J. Teunissen and U. Ebert, *J. Phys. D: Appl. Phys.*, **50**, 474001 (2017). https://doi.org/10.1088/1361-6463/aa8faf
11. O. Chanrion and T. Neubert, *J. Comput. Phys.*, **227**, No. 15, 7222–7245, (2008). https://doi.org/10.1016/j.jcp.2008.04.016
12. B. Bagheri, J. Teunissen, U. Ebert, et al., *Plasma Sources Sci. Technol.*, **27**, 095002, (2018). https://doi.org/10.1088/1361-6595/aad768
13. V. P. Pasko, in: M. Füllekrug, E. A. Mareev, and M. J. Rycroft, eds., *NATO Science Ser. II: Mathematics, Physics and Chemistry, V. 225. Sprites, Elves and Intense Lightning Discharges*, Springer, Dordrecht (2006), p. 253–311.
14. U. Ebert and D. D. Sentman, *J. Phys. D: Appl. Phys.*, **41**, No. 23, 230301 (2008).
15. G. A. Dawson and W. P. Winn, *Z. Phys.*, **183**, 159 (1965). https://doi.org/10.1007/BF01380792
16. I. Gallimberti, *J. Phys. D: Appl. Phys.*, **5**, 2179–2189 (1972). https://doi.org/10.1088/0022-3727/5/12/307
17. J. Qin and V. P. Pasko, *J. Phys. D: Appl. Phys.*, **47**, 435202 (2014). https://doi.org/10.1088/0022-3727/47/43/435202
18. S. Chen, R. Zeng, and C. Zhuang, *J. Phys. D: Appl. Phys.*, **46**, No. 37, 375203 (2013). https://doi.org/10.1088/0022-3727/46/37/375203
19. W. J. Yi and P. F. Williams, *J. Phys. D: Appl. Phys.*, **35**, No. 3, 205–218 (2002).
20. T. M. P. Briels, J. Kos, G. J. J. Winands, et al., *J. Phys. D: Appl. Phys.*, **41**, 234004 (2008). https://doi.org/10.1088/0022-3727/41/23/234004
21. G. V. Naidis, *Phys. Rev. E*, **79**, 057401 (2009). https://doi.org/10.1103/PhysRevE.79.057401
22. N. G. Lehtinen and N. Østgaard, *J. Geophys. Res.*, **123**, 6935–6953 (2018). https://doi.org/10.1029/2018JD028646
23. M. B. Zheleznyak, A. K. Mnatsakanyan, and S. V. Sizykh, *High Temp. Sci.*, **20**, No. 3, 357–362 (1982).
24. M. I. D'yakonov and V. Y. Kachorovskii, *Sov. Phys. JETP*, **68**, No. 5, 1070–1074 (1989).
25. S. V. Pancheshnyi, S. M. Starikovskaia, and A. Y. Starikovskii, *J. Phys. D: Appl. Phys.*, **34**, No. 1, 105–115 (2001). https://doi.org/10.1088/0022-3727/34/1/317
26. R. F. Harrington, *Field Computation by Moment Methods*, IEEE Press, New York (1993).
27. N. Y. Babaeva and G. V. Naidis, *IEEE Trans. Plasma Sci.*, **25**, 375–379 (1997). https://doi.org/10.1109/27.602514
28. V. P. Pasko, U. S. Inan, and T. F. Bell, *Geophys. Res. Lett.*, **25**, No. 12, 2123–2126 (1998). https://doi.org/10.1029/98GL01242

29. A. N. Lagarkov and I. M. Rutkevich, *Ionization Waves in Electrical Breakdown of Gases*, Springer-Verlag, New York (1994).

30. L. B. Loeb, *Science*, **148**, No. 3676, 1417–1426, (1965), https://doi.org/10.1126/science.148.3676.1417.

31. A. Y. Starikovskiy and N. L. Aleksandrov, *Plasma Sources Sci. Technol.*, **29**, 075004 (2020). https://doi.org/10.1088/1361-6595/ab9484

32. G. Derks, U. Ebert, and B. Meulenbroek, *J. Nonlinear Sci.*, **18**, 551–590 (2008). https://doi.org/10.1007/s00332-008-9023-0

33. M. I. D'yakonov and V. Y. Kachorovskii, *Sov. Phys. JETP*, **67**, No. 5, 1049–1054 (1988).

34. N. L. Aleksandrov and E. M. Bazelyan, *J. Phys. D: Appl. Phys.*, **29**, 740–752 (1996). https://doi.org/10.1088/0022-3727/29/3/035

35. V. P. Pasko, "Dynamic Coupling of Quasi-Electrostatic Thundercloud Fields to the Mesosphere and Lower Ionosphere: Sprites and Jets," PhD thesis, Stanford University, Stanford, CA (1996).

36. I. Gallimberti, *J. Phys. Colloques*, **40**, No. C7, 193–250 (1979). https://doi.org/10.1051/jphyscol:19797440